VOL. 15, NO. 13, JULY 2020 ISSN 1819-6608
ARPN Journal of Engineering and Applied Sciences

www.arpnjournals.com

CLASSICAL AND PREDICTIVE CONTROL APPLIED TO A NON-LINEAR SYSTEM OF COUPLED TANKS

German A. Pulido-Cortes, Alejandro Moreno-Artunduaga and Diego F. Sendoya-Losada
Department of Electronic Engineering, Faculty of Engineering, Surcolombiana University, Neiva, Huila, Colombia
E-Mail: diego.sendoya@usco.edu.co

ABSTRACT

In this work, two controllers, a Proportional Integral (PI) and a Model-based Predictive Controller (MPC), have been designed to regulate a non-linear liquid level system. First, the modeling and linearization of the system was performed using Taylor series. Then the PI controller was designed around a certain setpoint. Next, an algorithm was designed according to the Extended Prediction Self-Adaptive Control (EPSAC). Finally, the performance of the controllers is evaluated for setpoint tracking and disturbance rejection.

Keywords: EPSAC, Level control, MBPC, PI, RMSE.

1. INTRODUCTION

In almost all industrial process applications, the control of variables is critical to their safe and efficient operation. The most common controlled variables are pressure, level, temperature, and flow. Level control loops are very common in the industry, in fact they rank second after flow control loops. Due to the importance and the large number of processes that require precise level control, the Surcolombiana University has a system of coupled tanks called CE105 MV. As can be seen in Figure-1, this system presents a configuration similar to that found in many industrial applications or as part of a much larger and more sophisticated plant.

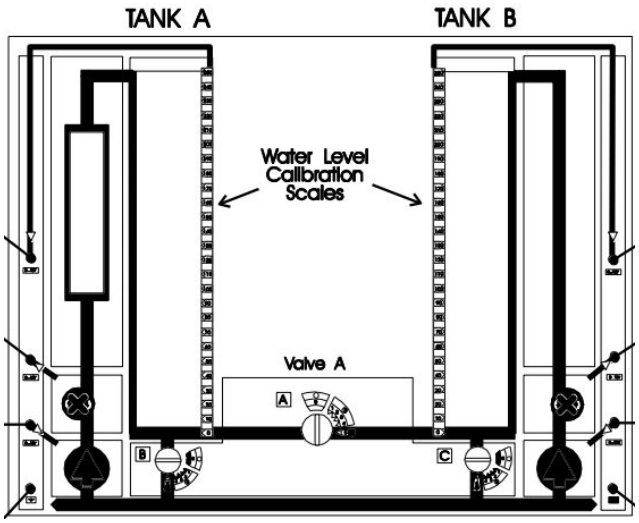

Figure-1. CE105MV System.

In general, the control of the liquid level in a system of coupled tanks is carried out by means of classical control techniques such as PI or PID, due to its known and simple structure [1]-[3]. For the design of these conventional controllers it is necessary to choose a setpoint and then find a linear model of the system, ensuring that the control works well in this region. When it moves away from the setpoint, the controller loses effectiveness [4]. In this contribution, Model-based Predictive Control (MPC) is applied to a system coupled tanks: CE105 MV [5]. For this document, a Single-Input Single-Output (SISO) configuration has been considered.
The MPC principle is simple. A model of the process is determined in advance, for example, by modeling or identification. With the help of this model, the process output is calculated with different inputs. The input that gives the best results is applied to the system, allowing to control processes with unusual dynamic behaviors, such as non-minimal phase, highly oscillatory, or unstable processes [6].

There is much documentation on classic and advanced control techniques applied to liquid level processes. In this contribution, the Extended Predictive Self-Adaptive Control (EPSAC) algorithm is used to setpoint tracking and disturbance rejection. Then a comparison is made with the classic PI control to demonstrate the effectiveness of the proposed algorithm. The performance of these controllers is tested and evaluated in a simulation environment. Simulation is done using Matlab®/Simulink® software.

2. MATERIALS AND METHODS

2.1 Process Model

MPC obviously requires a process model. The presented mathematical model is given by the equations that describe the complete system. Figure-2 shows their respective schematic. The dynamic model is determined by the relationship between the inlet flow Q_i and the outlet flow Q_c through the discharge valve. Equation (1) describes this relationship.

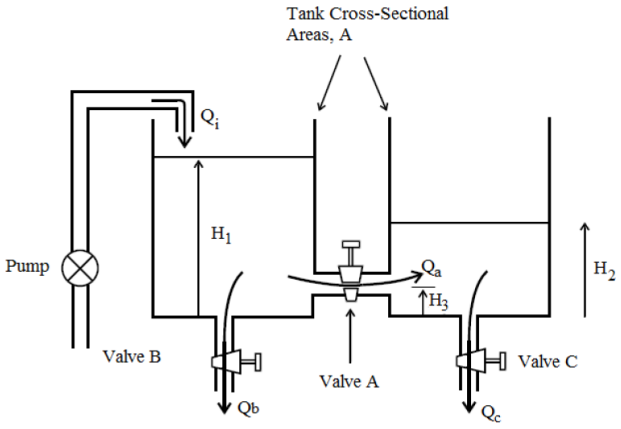

Figure-2. Schematic of coupled tanks.

$$Q_i - Q_a - Q_b = A\frac{dH_1}{dt} \quad (1)$$

$$Q_a - Q_c = A\frac{dH_2}{dt} \quad (2)$$

Valves are assumed to behave as a standard sharp-edged port [7], and the outflow through the discharge valve is related to the level of liquid in the tank by Equations (3), (4), and (5):

$$Q_a = aC_a\sqrt{2g(H_1 - H_2)} \quad (3)$$

$$Q_b = aC_b\sqrt{2gH_1} \quad (4)$$

$$Q_c = aC_c\sqrt{2gH_2} \quad (5)$$

A is the cross-sectional area of the tanks; a is the cross-sectional area of the valve orifice; C_a, C_b, and C_c are the discharge coefficients of the valves and g is the gravity constant. Combining Equations (1) to (5) gives:

$$Q_i = A\frac{dH_1}{dt} + aC_a\sqrt{2g(H_1 - H_2)} + aC_b\sqrt{2gH_1} \quad (6)$$

$$A\frac{dH_2}{dt} = aC_a\sqrt{2g(H_1 - H_2)} - aC_c\sqrt{2gH_2} \quad (7)$$

Equations (6) and (7) are first order nonlinear differential equations, to be useful in control systems, the equations must be linearized considering small variations on the desired operating fluid level in the tanks [8]. Applying the Taylor series and performing the Laplace transform, the transfer function of the system for coupled tanks is obtained:

$$G(s) = \frac{D_1}{s^2 + D_2 s + D_3} \quad (8)$$

$$D_1 = \frac{K_p C_a a\sqrt{2g}}{4A^2\sqrt{H_1 - H_2}}$$

$$D_2 = \frac{a\sqrt{2g}}{A}\left(\frac{C_b}{2\sqrt{H_1}} + \frac{C_a}{H'} + \frac{C_c}{2\sqrt{H_2}}\right)$$

$$D_3 = \frac{a^2 2g}{4A^2}\left(\frac{C_b C_a}{H'\sqrt{H_1}} + \frac{C_b C_c}{\sqrt{H_1}\sqrt{H_2}} + \frac{C_c C_a}{H'\sqrt{H_2}}\right)$$

$$H' = \sqrt{H_1 - H_2}$$

Table-1. System parameters [9].

Symbol	Description	Value
A	Cross-sectional area of the tanks	$9350\text{x}10^{-6}$ m^2
a	Cross-sectional area of the valve orifice	$78.50\text{x}10^{-6}$ m^2
C_a	Discharge coefficient of valve A	0.5
C_b	Discharge coefficient of valve B	0.2
C_c	Discharge coefficient of valve C	0.2
h_{max}	Maximum liquid level	0.25 m
v_{max}	Maximum input voltage	10 V
K_p	Pump gain	$6.66\text{x}10^{-6}$m^3/sV
K_h	Sensor level gain	40 V/m
g	Gravity constant	9.8 m/s^2

K_p is the pump gain and K_h is the sensor level gain in tank 2. The system parameters are shown in Table-1.

Finally, the transfer function is given by:

$$\frac{L(s)}{V(s)} = \frac{2.446.10^{-7}}{s^2 + 0.1695s + 1.9857.10^{-3}} \quad (9)$$

2.2 PI Controller Design

The following methodology was used to design the PI controller and test it through simulation (Figure-3).

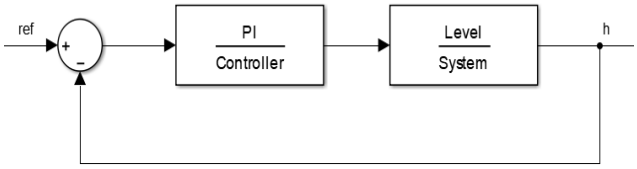

Figure-3. Schematic of PI control.

Due to the non-linear dynamics of the system, the scenario was set to design and test the PI controller. The design criteria was that the controlled system output had the minimum settling time, the closed loop response did not have overshoot, and that the PI controller output did not exceed 10 volts because this value is the maximum voltage allowed at the pump.

The algorithm that describes the behavior of the PI controller is:

$$u(t) = K_p e(t) + K_i \int_0^t e\,(t)d\tau \quad (10)$$

$u(t)$ is the output signal of the PI controller, which in this case corresponds to the voltage applied to the pump. $e(t)$ is the input signal of the PI controller, which is defined as $e(t) = r(t) - y(t)$, where $r(t)$ is the setpoint and $y(t)$ is the output of the process, that is, the level of liquid in the tank. K_p is the proportional gain and K_i is the integral gain.

Applying the Laplace transform, the transfer function of the PI controller is found:

$$U(s)/E(s) = K_p + K_i/s \quad (11)$$

A PI controller is designed so that the system adequately tracks a step input $h = 0.1$ m.

The transfer function of the PI controller is:

$$C(s) = \frac{U(s)}{E(s)} = \frac{85s+1.4}{s} \quad (12)$$

2.2 EPSAC

It is common practice in MBPC to structure the future control scenario. At each current moment t, the process output $y(t+k)$ is predicted over a time horizon $k = 1 \dots N_2$. The predicted values are indicated by $y(t+k|t)$ and the value N_2 is called the prediction horizon. The prediction model used is given in (7). The forecast depends on the past inputs and outputs, but also on the future control scenario $u(t+k|t)$ with $k = 0 \dots N_2 - 1$. This can be done by defining a control horizon N_u with $1 \le N_u \le N_2$, after which the control strategy remains constant, i.e. $u(t+k|t) = u(t+N_u-1|t)$ for $N_u \le k \le N_2 - 1$.

Conceptually the future response $y(t+k|t)$ can be considered as the cumulative result of 2 effects: $y_{base}(t+k|t)$, which is calculated based on the effect of future disturbances $n(t+k|t)$, the effect of past control $u(t-1)$, $u(t-2)$, … and the effect of a basic future control scenario $u_{base}(t+k|t)$ with $k = 0 \dots N_2 - 1$; and $y_{opt}(t+k|t)$, which is the effect of the optimizing future control actions $\delta u(t+k|t)$ with$k = 0 \dots N_2 - 1$, i.e. $\delta u(t+k|t) = u(t+k|t) - u_{base}(t+k|t)$, where $u(t+k|t)$ is the optimal control input that is sought.

Structuring leads to simplified calculations by reducing the degrees of freedom of the control vector from N_2 to N_u and generally has a positive effect on robustness. The extremely simplified version $N_u = 1$ leads to remarkably good results in many practical applications. Hence, a control horizon $N_u = 1$ is used in this work. The control horizon implies that $u_{base}(t+k|t) = u_{base}(t|t)$ and $\delta u(t+k|t) = \delta u(t|t)$ for $1 \le k \le N_2 - 1$. Furthermore, $y_{opt}(t+k|t)$ —being the result of $\delta u(t+k|t)$— is the effect of a single step input with amplitude $\delta u(t|t)$ at time t. The system output at time $t+k$ is thus, $y_{opt}(t+k|t) = g_k \delta u(t|t)$ for $1 \le k \le N_2$, where g_k for $k = 1 \dots N_2$ are the coefficients of the unit step response of the system.

For a linear system with constant parameters, the step response coefficients are constant and thus must be calculated only once. Using matrix notation, $Y_{opt} = GU$:

$$\begin{bmatrix} y_{opt}(t+1|t) \\ y_{opt}(t+2|t) \\ \dots \\ y_{opt}(t+N_2|t) \end{bmatrix} = \begin{bmatrix} g_1 \\ g_2 \\ \dots \\ g_{N_2} \end{bmatrix} \delta u(t|t) \quad (13)$$

The key EPSAC equation is then $Y = Y_{base} + Y_{opt}$. The task of the controller is to find the control vector $u(t+k|t)$ with $k = 0 \dots N_2 - 1$ that minimizes the cost function:

$$\sum_{k=N_1}^{N_2} [r(t+k|t) - y(t+k|t)]^2 = (R-Y)^T(R-Y) \quad (14)$$

where the default value for N_1 is the systems time delay ($N_1 = 1$). $r(t+k|t)$ is the reference trajectory, which is in this case the setpoint R. Minimization of (9) with respect to U gives the optimal solution:

$$U^* = (G^T G)^{-1} G^T (R - Y_{base}) \quad (15)$$

Since the control horizon is chosen $N_u = 1$, the matrix $G^T G$ with dimensions $N_u \times N_u$ is a scalar and thus its inversion has a low computational cost. The actual control action applied to the real process at the current time t is $u(t) = u_{base}(t|t) + \delta u(t|t)$, i.e.:

$$u(t) = u_{base}(t|t) + U^*(1) \quad (16)$$

At the next sampling instant $t+1$, the whole procedure is repeated by considering the new measurement information $y(t+1)$ (so-called receding horizon).

Clipping is applied to the control action whenever necessary because the maximum input voltage is 10 V and the minimum value is 0 V.

3. RESULTS AND DISCUSSIONS

The simulation was conducted towards three scenarios to compare the behavior of the PI and EPSAC algorithms. The performance of the controllers is evaluated for the response at the selected setpoint ($H_2 = 0.1$), the tracking to a reference level, and the effective rejection of the disturbances.

3.1 SCENARIO 1: Response at the setpoint

To verify the performance of the controllers at the selected operating point, an input $H_2 = 0.1$ is applied to the system and the response presented in Figure-4 is obtained.

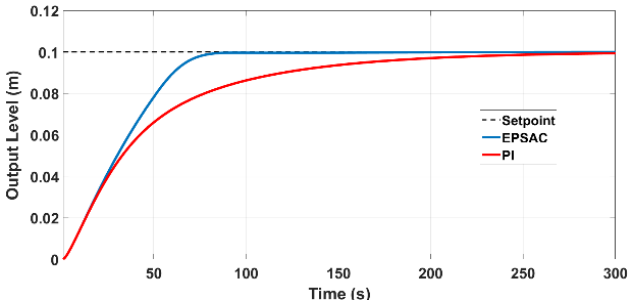

Figure-4. Response with PI and EPSAC.

The response of the controllers presents great differences in terms of speed, where the EPSAC algorithm is visibly faster stabilizing at 65 seconds, while the PI controller reaches the steady state at 166 seconds. It is also possible to establish that for the selected setpoint $H_2 = 0.1$, both controllers do not present an overshoot.

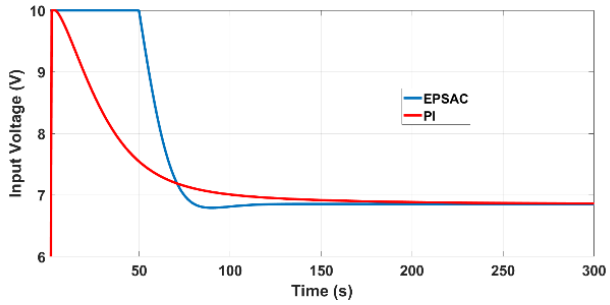

Figure-5. Process input for test at setpoint.

The control actions exerted on the process can be visualized in Figure-5. The EPSAC algorithm takes the plant to its maximum capacity (10V) for 50 seconds, to subsequently decrease the input voltage to 6.85V. For its part, the PI controller reduces the input voltage gently, which slows down the response of the plant under its influence.

3.2 SCENARIO 2: Disturbance Rejection

The system is disturbed by increasing the discharge coefficient of tank 2. Time after the plant reaches steady state with a reference level of $H_2 = 0.1$ and the discharge coefficient $C_c = 0.2$ is changed to 0.3 as shown in Figure-6. When both controllers manage to completely reject the disturbance after 700 seconds, the discharge coefficient is again reset to 0.2.

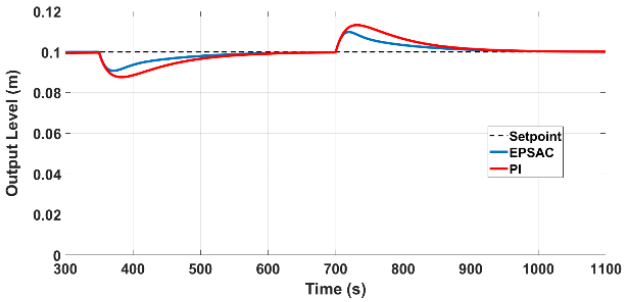

Figure-6. Disturbance rejection with PI and EPSAC.

The EPSAC algorithm and the PI controller manage to reject the first disturbance at 418 sec and 472 sec respectively as shown in Figure-6. The controller implemented with the EPSAC algorithm exerts greater control force (Figure-7), so it manages to recover more quickly than the PI controller. In the case when the disturbance has ended and the system returns to the original discharge coefficient, EPSAC recovers 52 seconds before the PI.

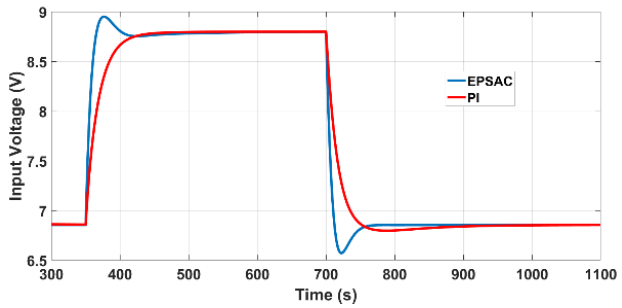

Figure-7. Input process for disturbance rejection with PI and EPSAC algorithms.

3.3 SCENARIO 3: Setpoint Tracking

To evaluate the behavior of the closed-loop system at different points of operation, step-type signals are entered starting at 0.04 m with increases of 0.04 until reaching 0.16 m. Figure-8 presents the results obtained at the output of tank 2, where EPSAC has a prediction horizon $N_2 = 56$.

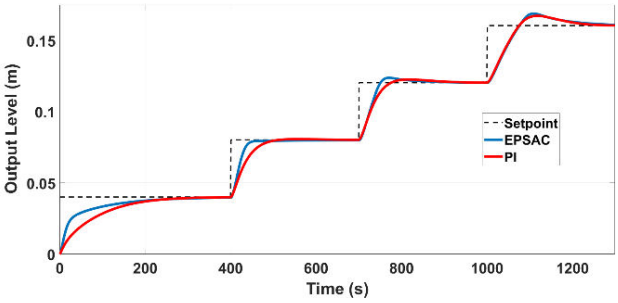

Figure-8. Setpoint tracking with PI and EPSAC.

EPSAC in the first three setpoint follow-up tests (0.04, 0.08 and 0.12 m) achieves shorter settling times than the PI controller, becoming up to 7.3% faster at best ($H_2 = 0.12$). In tests that were performed with input values above the setpoint, both controllers begin to show overshoot. Even for the last step (0.16 m), PI achieves better results by stabilizing 66 seconds before the EPSAC algorithm. This behavior can be better understood when analyzing Figure-9, since for the last step the control actions present very similar forms where the smoothness of the PI controller response offers the afore mentioned benefits.

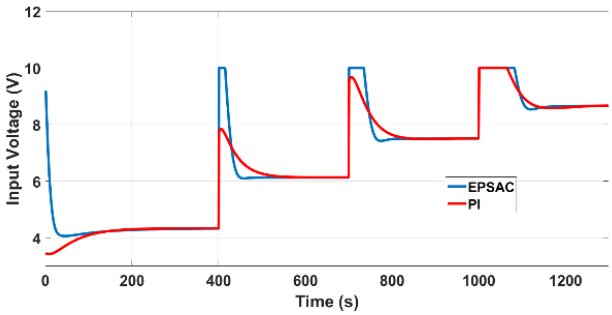

Figure-9. Input process with PI and EPSAC algorithms.

The EPSAC algorithm always brings the plant to its maximum capacity (10V) in the first seconds, thanks to this it achieves excellent results in terms of speed compared to the PI controller.

To have a more precise comparison of both control strategies, the Root Mean Square Error (RMSE) variation was applied to the 3 proposed scenarios.

$$RMSE = \sqrt{\frac{\sum_{t=1}^{N}[r(t)-y(t)]^2}{N}} \quad (17)$$

where $r(t)$ is the setpoint signal, $y(t)$ is the output signal, and N is the number of samples. Table-2 shows the RMSE variations for both the PI and EPSAC algorithms when the three simulation scenarios are applied.

Table-2. RMSE Variations for PI and EPSAC algorithms.

Scenario	PI%	EPSAC%
1	2.89	2.64
2	0.54	0.34
3	1.15	0.99

According to Table-2, the EPSAC algorithm presents a better performance according to the RMSE, being very low compared to the PI for the three test scenarios.

4. CONCLUSIONS

In this work, the performance of the EPSAC algorithm and the PI control strategy were evaluated. In all tests, EPSAC showed great superiority both in disturbance rejection and setpoint tracking. This is because EPSAC uses a linearized model of the process to make predictions of future behavior and with this adjust the control action that it will apply.

REFERENCES

[1] J. F. Caipa-Roldán, J. M. Salamanca and J. L. Rodríguez-Herrera. 2010. Control digital de nivel para sistema de tanques interconectados mediante servo-válvula. Ingeniería Investigación y Desarrollo. 10(1): 55-63.

[2] V. Bhambhani and Y. Q. Chen. 2008. Experimental study of fractional order proportional integral (FOPI) controller for water level control. 47th IEEE Conference on Decision and Control.

[3] E. Govinda-Kumar and J. Arunshankar. 2018. Control of nonlinear two-tank hybrid system using sliding mode controller with fractional-order PI-D sliding surface. Computers & Electrical Engineering. 71: 953965.

[4] D. F. Sendoya-Losada. J. O. Arroyave-Quezada, and A. J. Velasquez-Pobre. 2019. EPSAC and NEPSAC algorithms applied to a nonlinear liquid level system. 4th IEEE Colombian Conference on Automatic control (CCAC).

[5] D. F. Sendoya-Losada, D. C. Vargas-Duque and I. J. Ávila-Plazas. 2018. Implementation of a neural control system based on PI control for a nonlinear process. 1st IEEE Colombian Conference on Applications in Computational Intelligence.

[6] R. De Keyser. 2003. A 'Gent'le approach to predictive control. UNESCO Encyclopedia of Life Support Systems (EoLSS), Eolss Publishers Co Ltd, Oxford.

[7] Ogata Katsuhito. 1987. Dinamica de sistemas, Prentice Hall, Mexico.

[8] H. Bastidas, P. Ponce, R. Ramírez and A. Molina. 2013. Model and Control for coupled tanks using Labview. International Conference on Mechatronics, Electronics and Automotive Engineering.

[9] TecQuipment. 2016. CE105 and CE105MV Coupled Tanks user manual. TecQuipment Ltd.

[10] Denuth H. and M. Beale. 1996. Neural network toolbox user's guide for use with Matlab. The Math Works Inc., Marde.

[11] Sendoya D. F. 2013. ¿Qué es el control predictivo y hacia dónde se proyecta? Publicaciones e Investigación. 7, pp.53-59.

[12] Sendoya-Losada, D. F., Faiber Robayo Betancourt, and José Salgado Patrón. 2017. Application of a predictive controller with variable time delay ingeneral anesthesia. ARPN Journal of Engineering and Applied Sciences. 12(8): 2661-2667.

[13] Sendoya-Losada, Diego F. and Johan Julián Molina Mosquera. 2017. Linear and nonlinear predictive control algorithms applied to a heated tank system. ARPN Journal of Engineering and Applied Sciences. 12(23): 6895-6903.

[14] Sendoya-Losada, D. F. 2019. Principles, applications and perspectives of predictive control. ARPN Journal of Engineering and Applied Sciences. 14(13): 2464-2467.